Water Molecule Interactions

D. HANKINS AND J. W. MOSKOWITZ*
Chemistry Department, New York University, Washington Square College, New York, New York 10003
AND
F. H. STILLINGER†
Bell Telephone Laboratories, Incorporated, Murray Hill, New Jersey 07974

(Received 17 August 1970)

Accurate SCF calculations have been carried out to investigate the potential of interaction for pairs and triplets of water molecules. The most stable pair configuration involves a linear hydrogen bond of length $R_{OO}=3.00$ Å and strength 4.72 kcal/mole. Three-molecule nonadditivities are large in magnitude and vary in sign according to the hydrogen-bond pattern involved. In both aqueous liquids and solids, the net trimer nonadditivity effect amounts to increased binding energy, decreased neighbor distance, and slightly enhanced tendency toward perfect tetrahedral coordination symmetry. The nonadditivity furthermore is inconsistent with the phenomenology of simple mutual electrostatic polarization between neighboring molecules.

I. INTRODUCTION

The local structure that is peculiar to liquid water and aqueous solutions plays a fundamental role in diverse chemical, biological, and meteorological phenomena. A variety of statistical-mechanical techniques is now available for study of liquids, including water, but an indispensable ingredient for their application is the relevant intermolecular potential function. We are therefore fortunate that computational quantum mechanics has progressed to a point where systematic and reasonably precise calculations of the potential energy for small groups of water molecules have become possible. It has thus become likely that we shall soon achieve a comprehensive understanding of the nature and the effects of structure in aqueous fluids.

Morokuma and Pederson[1] were the first to carry out *ab initio* Hartree–Fock calculations for a pair of interacting water molecules. Their Gaussian basis, however, was quite small. More recently, Kollman and Allen[2] repeated the dimer calculation with a more extensive Gaussian basis and have obtained substantially smaller hydrogen-bond energies. Morokuma and Winick[3] have also carried out water molecule pair interaction calculations in a minimal Slater basis. Below we shall provide detailed comparison of all such calculations that are currently available.

In a collection of N interacting water molecules, the total energy $E(\mathbf{x}_1\cdots\mathbf{x}_N)$ clearly depends upon the nuclear configuration vectors $\mathbf{x}_j$ for all of the molecules. It is convenient to decompose E into single-molecule energies $E^{(1)}$, pair interactions $V^{(2)}$, specific triplet contributions $V^{(3)}$, etc., so that finally E may be expressed as follows:

$$E(\mathbf{x}_1\cdots\mathbf{x}_N)=\sum_{i=1}^{N}E^{(1)}(\mathbf{x}_i)+\sum_{i<j=1}^{N}V^{(2)}(\mathbf{x}_i,\mathbf{x}_j)+\sum_{i<j<k=1}^{N}V^{(3)}(\mathbf{x}_i,\mathbf{x}_j,\mathbf{x}_k)+\cdots+V^{(N)}(\mathbf{x}_1\cdots\mathbf{x}_N). \tag{1.1}$$

The function $E^{(1)}$ is clearly an isolated molecule property; $V^{(2)}$, $V^{(3)}$,$\cdots$ may then be obtained recursively by considering the energy of sets of two, three,$\cdots$ molecules, and performing the requisite subtractions:

$$\begin{aligned}E^{(1)}(\mathbf{x}_i)&\equiv E(\mathbf{x}_i),\\ V^{(2)}(\mathbf{x}_i,\mathbf{x}_j)&=E(\mathbf{x}_i,\mathbf{x}_j)-E^{(1)}(\mathbf{x}_i)-E^{(1)}(\mathbf{x}_j),\\ V^{(3)}(\mathbf{x}_i,\mathbf{x}_j,\mathbf{x}_k)&=E(\mathbf{x}_i,\mathbf{x}_j,\mathbf{x}_k)-E^{(1)}(\mathbf{x}_i)-E^{(1)}(\mathbf{x}_j)\\ &\quad-E^{(1)}(\mathbf{x}_k)-V^{(2)}(\mathbf{x}_i,\mathbf{x}_j)-V^{(2)}(\mathbf{x}_i,\mathbf{x}_k)-V^{(2)}(\mathbf{x}_j,\mathbf{x}_k),\\ &\vdots\end{aligned} \tag{1.2}$$

By virtue of the large dipole moment of the water molecule, one would expect that electrostatic polarization effects between neighbors would alone ensure substantial contributions to $V^{(3)}$ at least, if not to $V^{(4)}$, $V^{(5)}$, etc.

The primary objective of this paper is study of the pair potential $V^{(2)}$ and the leading nonadditivity quantity $V^{(3)}$.[4] We have consistently striven to use the largest practicable set of Gaussian basis functions to describe the molecular orbitals since the dispersion in previously published $V^{(2)}$ results[1–5] is unacceptably wide. Our present $V^{(2)}$ and $V^{(3)}$ calculations are probably close to the Hartree–Fock limit; it is vital to establish this limit to calibrate further less accurate calculations on larger groups of molecules, as well as to provide a firm basis upon which to estimate correlation effects quantitatively.

Section II is devoted to the single water molecule, and the basis functions utilized throughout this project are specified there. It is important to note that this basis includes d functions for oxygen atoms, as well as hydrogen atom p functions, both of which seem to be important for quantitative description of hydrogen bonding. Single-molecule properties calculated with this basis are listed in Sec. II.

The same basis functions are applied in Sec. III to each of a pair of interacting water molecules. In order to

TABLE I. Contracted Gaussian basis [531 | 21] for water.

Atom	Type	Approximate orbital representation	Basis functions[a]
O	s	$1s$	0.243991(31.31660)+0.152763(76.2320)
		$1s'$	0.904785(290.785)+0.121603(1424.0643) +0.029225(4643.4485)
		$1s''$	0.264438(4.60390)+0.45824(12.86070)
		$2s$,	1.05134(0.93110)−0.140314(9.7044)
		$2s'$	1.0(0.28250)
	p	$2p$	0.124190(7.90403)+0.019580(35.18320) +0.394730(2.30512)
		$2p'$	1.0(0.21373)
		$2p''$	1.0(0.71706)
	d	$3d$	1.0(0.897)
H	s	$1s$	0.817238(0.65341)+0.231208(2.89915) +0.032828(19.24060)
		$1s'$	1.0(0.17758)
	p	$2p$	1.0(0.9650)

[a] Linear combinations are written in the form $C_1(\alpha_1)+C_2(\alpha_2)+\cdots$, where C's are coefficients and α's are the Gaussian exponents. The linear combinations shown in the table are unnormalized.

specify the pair potential $V^{(2)}$, one must in principle span a 12-dimensional unbounded region in the relative configuration space for the six nuclei. Of course, practical considerations force one to be very selective in which configurations to examine, especially under a commitment to use a large, slow-running, and expensive, basis set. For the most part, our molecule-pair calculations used the stable monomer geometry obtained in Sec. II, and concentrated on those relative configurations which should occur with high frequency between nearest neighbors in liquid water. To the extent that comparisons with previous work are possible, one finds that $V^{(2)}$ is rather poorly predicted unless an extensive basis set is used.

The three-molecule computations (which are relevant to $V^{(3)}$) are reported in Sec. IV. The class of possible triplet configurations is indeed vast, and more than before we have been forced to be stringently selective. Once again we have tried to examine cases with maximum relevance to the hydrogen-bond networks that

TABLE II. Properties of water monomer from reported *ab initio* wavefunctions.

	R_{OH}[a]	∢HOH	Energy[b]	Dipole moment[c]	α_{xx}[d]	α_{yy}	α_{zz}	$\frac{1}{3}\mathrm{Tr}(\alpha)$
This work, [531 | 21][e]	0.945	106°	−76.041582	2.190				
Morokuma and Pederson, (53 | 3), Ref. 1	0.959	113°	−75.54939					
Kollman and Allen, [31 | 1], Ref. 2	0.967	110°	−75.97565	2.480				
Morokuma and Winick, Ref. 3	0.9819	101.07°	−75.705032					
Del Bene and Pople, [21 | 1], Ref. 5	0.992	100.05°	−75.500133	1.820				
Neumann, Moskowitz, and Liebmann, [532 | 21], Refs. 11, 14			−76.04403	2.092	1.226	1.651	1.452	1.443
Diercksen, [541 | 31], Ref. 13	0.9443	105.3°	−76.05326					
Experiment	0.9572	104.52°	−76.481[f]	1.86				1.444

[a] In angstroms.
[b] In atomic units.
[c] In debyes.
[d] In 10^{-24} cm^3 = 6.74855 a.u.
[e] See Ref. 23 of Ref. 11 for explanation of notation.
[f] The Hartree–Fock limit is −76.089 (see Ref. 11, Table VI).

occur in condensed phases. Our $V^{(3)}$ results confirm the notion of cooperativity in hydrogen-bond formation energies,[4–7] and they suggest that many-body interactions provide an over-all compressive effect in condensed phases. They also indicate that $E^{(1)}$ and $V^{(2)}$ are more sensitive to basis size than $V^{(3)}$, $V^{(4)}$, $\cdots$.

A major portion of the statistical-mechanical theory of liquids is based upon an assumption of pairwise additivity for the over-all potential of interaction (i.e., $V^{(j)}=0$ for $j\geq 3$). In particular, this is especially convenient for "Monte Carlo"[8] or "molecular dynamics"[9] simulations of the liquids of interest by computer. We know now that this is manifestly invalid for water, in the strict sense. Still, a variational principle may be utilized to construct an "effective pair potential" that optimally reproduces the true local order in the liquid.[10] We believe that our present results, and those of like character which will surely follow in the near future, will provide important guides to the intelligent use of these effective pair potentials in computer simulations of aqueous fluids.

The final Sec. V discusses several important issues. Among them are the neglected effects of electron correlation, the relation of our $V^{(3)}$ results to electrostatics, and a set of open problems that deserve the attention of future research.

II. COMPUTATIONAL PROCEDURE AND MONOMER PROPERTIES

All of the calculations to be reported here for energies, wavefunctions, and molecular properties were performed on the New York University CDC6600 Computer, using the Polyatom programs. An extensive Gaussian basis was selected to represent each monomer; it consists of 30 functions derived by contraction from 45 primitives. Accordingly, the dimer calculations involve 60 independent functions, and the trimer calculations involve 90. This basis will be denoted by [531 | 21], following the notation introduced by Neumann and Moskowitz,[11] and it is very similar to the contracted basis [532 | 21] that they used to calculate water-molecule one-electron properties. The exponents required for the oxygen d-electron and hydrogen p-electron polarization functions were obtained by optimizing each exponent separately in the monomer. The LCAO MO self-consistent field calculations were carried out by Roothaan's procedure for closed shells.[12]

Except for a few cases that will be clear by their context, the equilibrium monomer geometry was retained in the dimer and trimer calculations. The indications are that deviations from this convention are rather small.

The first step in our computational program naturally was a detailed study of the isolated monomer with our [531 | 21] basis. The minimum energy obtained with this basis was -76.041582 a.u. corresponding to OH bonds of length 0.945 Å, and an angle of 106° between the bonds. Table I provides the coefficients and exponents that appear in [531 | 21], while Table II compares its monomer energy and stable configuration with those of other recent calculations,[1–3,5,11,13] that have been employed in water-molecule interaction studies. Liebmann[14] has used the Neumann–Moskowitz [532 | 21] basis to calculate diagonal elements of the polarizability tensor, and we include his results

TABLE III. One-electron properties[a] for the wavefunctions [531 | 21], [532 | 21], and (1062 | 42).

	[531 | 21]	[532 | 21]	(1062 | 42)
Dipole moment[b]			
μ_z	0.8719	0.823	0.785
Second moment[c]			
Q_{xx}	−5.444	−5.469	−5.563
Q_{yy}	−3.069	−3.050	−3.108
Q_{zz}	−4.359	−4.339	−4.416
Quadrupole moment[c]			
θ_{xx}	−1.730	−1.776	−1.801
θ_{yy}	1.833	1.855	1.882
θ_{zz}	−0.1026	−0.0788	−0.0805
Third moment[d]			
R_{xxz}	0.022	−0.049	−0.157
R_{yyz}	1.679	1.680	1.673
R_{zzz}	0.792	0.625	0.397
Octupole moment[d]			
Ω_{xxz}	−1.191	−1.250	−1.349
Ω_{yyz}	2.951	3.072	3.227
Ω_{zzz}	−1.760	−1.822	−1.878
Potential[e]			
at O	−22.334	−22.334	−22.329
Potential			
at H	−1.004	−1.007	−1.001
Electric field[f]			
E_z at O	−0.070	−0.060	−0.010
Electric field			
E_z at H	0.001	0.001	−0.002
Electric field			
E_y at H	0.009	0.007	0.000
Field gradient[g]			
q_{xx} at O	1.941	1.905	1.852
q_{yy} at O	−1.773	−1.736	−1.679
q_{zz} at O	−0.168	−0.169	−0.173

[a] All values are in atomic units. Precise definitions of the relevant operators appear in Ref. 11. The z axis points along the HOH-angle bisector, the y axis lies in the molecular plane, and the x axis is perpendicular to that plane. Unless otherwise stated, these results refer to an origin at the molecular center of mass ($x=y=0$, $z=0.1226$ a.u.).

[b] 1 a.u. = 2.541539 D. The experimental value is 0.7318 a.u.

[c] 1 a.u. = 1.344911×10^{-26} esu·cm².

[d] 1 a.u. = 0.711688×10^{-34} esu·cm³.

[e] 1 a.u. = 9.07618 esu/cm (or statvolt).

[f] 1 a.u. = 0.171524×10^{8} dyn/esu.

[g] 1 a.u. = 0.324123×10^{16} esu/cm³ (or statvolt/cm²).

TABLE IV. Dimer total energies and pair potentials.[a]

θ (deg)	$R_{O_2H_3}$ (Å)	$R_{O_1O_2}$ (Å)	∢HOH (deg)	$E(1,2)$ (a.u.)	$V^{(2)}(1,2)$ (kcal/mole)
0	0.945	3.00	106	−152.090159	−4.391
25	0.945	3.00	106	−152.090545	−4.633
40	0.945	3.00	106	−152.090691	−4.725
48	0.945	3.00	106	−152.090662	−4.707
70	0.945	3.00	106	−152.090093	−4.349
−30	0.945	3.00	106	−152.089581	−4.028
−40	0.945	3.00	106	−152.089286	−3.843
−54.7	0.945	3.00	106	−152.088638	−3.434
−70	0.945	3.00	106	−152.087558	−2.758
40	0.945	2.76	106	−152.089482	−3.966
40	0.945	2.88	106	−152.090492	−4.600
40	0.952	2.76	106	−152.089209	−3.795
40	0.963	2.76	106	−152.089451	−3.946
40	0.952	3.00	106	−152.090666	−4.709
40	0.960	3.00	106	−152.090529	−4.623
−54.7	0.945	2.76	106	−152.086987	−2.400
−54.7	0.945	2.90	106	−152.088332	−3.244
−54.7	0.945	3.15	106	−152.088527	−3.366
−54.7	0.945	3.39	106	−152.087742	−2.874
54.7	0.945	2.76	106	−152.089276	−3.837
54.7	0.945	2.76	[107 acceptor / 106 donor]	−152.089288	
54.7	0.945	2.76	[108 acceptor / 106 donor]	−152.089247	

[a] The configurations all refer to Fig. 1.

(which are in good agreement with experiment) in Table II for completeness.

A large number of one-electron properties for our wavefunction are arrayed in Table III. Displayed there as well are corresponding values for the Neumann–Moskowitz wavefunctions [532 | 21] and (1062 | 42).

Force constants for the single OH bond stretch, and the pure bend motions have been obtained by parabolic fit to the potential curves under the action of small nuclear displacements. These quantities are required for later comparison with the dimer properties. The result for stretch is 8.36×10^5 dyn/cm, and for bend 0.492×10^5 dyn/cm.

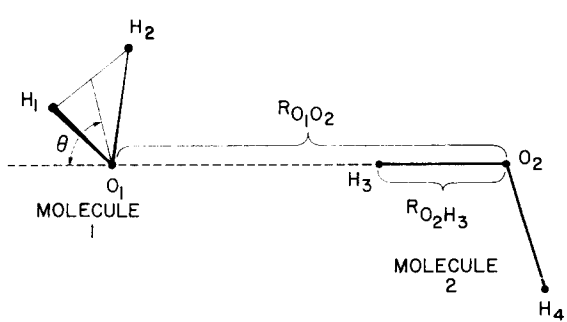

FIG. 1. Linear hydrogen-bonded water dimer. Molecule 2 lies entirely in the symmetry plane for the pair. Angle θ is positive for the *trans* configuration shown, and is negative for the analogous *cis* configuration.

The electron density in the monomer may be partially revealed by a Mulliken[15] population analysis. The gross atomic populations implied by our [531 | 21] basis are 8.6465 and 0.67675 for oxygen and hydrogen, respectively. More information about the electron distribution is conveyed by the density contours in various planes. Although contour maps probably have limited value in explaining details of hydrogen bonding between pairs of water molecules, one can reasonably expect that their features would strongly reflect the nature of the potential between a noble-gas atom and a water molecule in its detailed dependence upon direction of approach. We note in passing (from a study of monomer density maps) that considerable electron density occurs between the nominal bond directions,[16] and that lone-pair electrons fail to manifest distinctive directionality at the back of the molecule.

III. DIMER CALCULATIONS

The principal characteristic features of the water molecule pair potential $V^{(2)}$ stem from the ability to

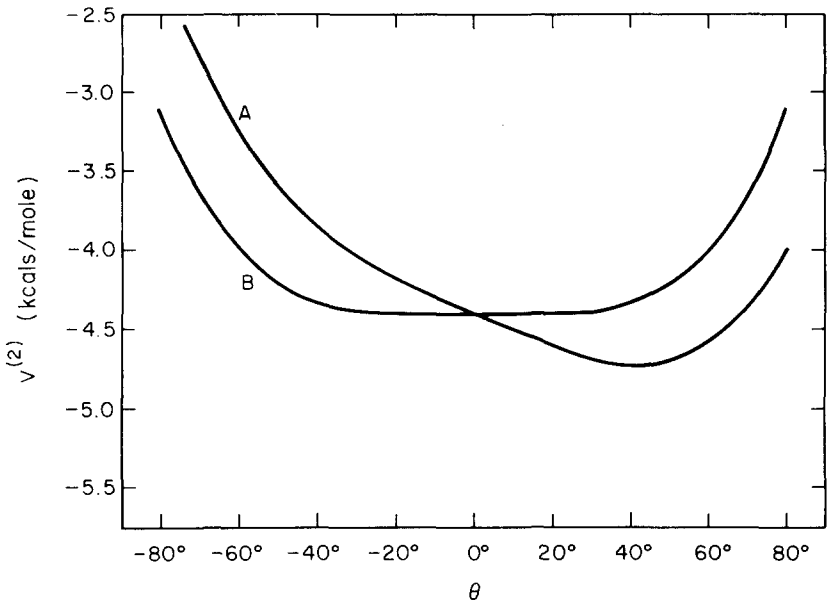

FIG. 2. Angle variation of $V^{(2)}$ for linear hydrogen bonds of length $R_{O_1O_2}=3.00$ Å. Curve A refers to the symmetric dimer shown in Fig. 1, while curve B involves rotation of the proton donor (molecule 2 in Fig. 1) by $\pm 90°$ about the hydrogen-bond axis.

form hydrogen bonds. Crystallographic studies of the ice polymorphs[17] and of the clathrate hydrates[18] strongly suggest that a single, essentially linear, hydrogen bond is the preferred mode of interaction. Recent *ab initio* quantum-mechanical calculations[1–5,13,19] agree, and furthermore suggest that the minimum energy configuration for the pair (dimer) should exhibit a plane of symmetry, and should have nonbonded protons *trans* to each other.

Figure 1 shows the relevant geometry. The results of a search for the most strongly bound configuration, and for the character of the $V^{(2)}$ surface in its neighborhood, are provided by Table IV. For the most part its entries correspond to undistorted monomers. We find that the $V^{(2)}$ minimum occurs when $R_{O_1O_2}=3.00$ Å, and $\theta=40°$. Furthermore no perceptible stretch in $R_{O_2H_3}$ arises at this minimum, although the monomer force constant for this single stretch (8.36×10^5 dyn/cm) decreases to 3.75×10^5 dyn/cm in the dimer.[20]

Table V compares our $V^{(2)}$ minimum (for undistorted monomers) with the analogous results of other *ab initio* calculations. Notice in particular the wide variance in θ, and the fact that small functional bases seem to imply small $R_{O_1O_2}$ and large binding energies. In this connection it is wise to bear in mind that small-basis calculations commit errors of several hundred kcal/mole in the ground-state energy compared to the Hartree–Fock limit solution, and this energy defect arises primarily from an inadequate wavefunction near the oxygen nucleus. One such poorly described molecule can then utilize the tails of orbitals centered on a neighboring molecule to improve its own oxygen core distribution. In view of the energies involved, the stage is set for a powerful (but spurious) extra attraction between the molecules. The net result would inevitably be smaller distances and stronger bonds predicted with small bases, compared to the exact Hartree–Fock result.

Water molecules manifest a universal tendency toward local tetrahedral coordination in condensed phases. This is quite clear from known crystal structures,[17,18] but it applies as well in the liquid[21] after due account is given the necessity of local strains and defects in the random hydrogen-bond network. It is therefore of interest to see if $V^{(2)}$ explicitly shows tetrahedral directionality.

Figure 2 presents two angle variation curves that were selected to probe this possibility. Both involve linear hydrogen bonds of length $R_{O_1O_2}=3.00$ Å. Curve A is the θ variation of $V^{(2)}$ for the reflection-symmetric configuration shown in Fig. 1. Consistent

TABLE V. Geometric parameters for the minimum-energy dimer according to various *ab initio* computations.

	$R_{O_1O_2}$ (Å)	θ (deg)	$\Delta R_{O_2H_3}$ (Å)	$V^{(2)}$ (kcal/mole)
This work, [531 | 21]	3.00	40	0.00	−4.72
Morokuma and Pederson (53 | 3), Ref. 1	2.66	0	0.012	−12.6
Kollman and Allen, [31 | 1], Ref. 2	3.0	25	0.01	−5.3
Morokuma and Winick, Ref. 3	2.78	54	0.0026	−6.55
Del Bene and Pople, [21 | 1], Ref. 5	2.73	58		−6.09
Diercksen, [541 | 31], Ref. 13	2.98			−4.83

with previous remarks, its minimum lies at $\theta=40°$. Curve B (see Table VI) is the analogous result for an asymmetric pair that may be obtained by rotating molecule 2 in Fig. 1 by $\pm 90°$ about the linear hydrogen-axis. The marked asymmetry of curve A stems from the difference in repulsion between protons not involved in the hydrogen bond in passing from *cis* to *trans* configurations. This distinction is not present for curve B, which is therefore precisely symmetric about $\theta=0$.

It is conceivable that curves A and B could have displayed a tendency toward tetrahedral directionality by having relative minima near $\theta=\pm 54°44'$ (the ideal tetrahedral angles). Figure 2, however, shows that clearly not to be the case. Curve B has a very small maximum at $\theta=0°$, though the degree to which this is true lies dangerously close to our roundoff error. It is widely known[22] that full hybridization of the $2s$ and $2p$ valence orbitals for first-row elements leads to tetrahedrally directed bond orbitals that have relevance, for instance, to the geometry of saturated hydrocarbons. Our present evidence indicates, however, that hybridization is quite incomplete in water. The reasons for local tetrahedral order in condensed aqueous phases evidently lie deeper in the quantum mechanical and statistical mechanical theory.

TABLE VI. Dimer energies at $R_{OO}=3.00$ Å, with 90° rotation of donor in Fig. 1 about the H bond.

θ (deg)	$V^{(2)}(1,2)$ (kcal/mole)
0	−4.3839
±25	−4.3852
±40	−4.326
±54.7	−4.121
±70	−3.644

Frank[6,7] has argued that hydrogen-bond formation in water is cooperative: After the first bond is established in an initially unbonded assembly of water molecules, subsequent contiguous bonds are stronger. This phenomenon is associated largely with potential nonadditivity (i.e., with the character of $V^{(3)}$, $V^{(4)}$, etc.), and will be examined in the next section. One aspect of cooperativity already arises in the dimer, in connection with the failure of monomers to achieve full sp^3 hybridization. The last entries in Table IV upon interpolation show that the proton acceptor (molecule 1 in Fig. 1) increases its bond angle by 0.5° upon formation of the hydrogen bond, when the angle θ of attack is itself tetrahedral (+54°44′). Evidently the partial covalency of the hydrogen bond in this configuration acts to enhance the degree of hybridization toward the full sp^3 limit. Since the acceptor molecule angle increases slightly from its monomer value (106°) toward the tetrahedral value ($2\times 54°44'=109°28'$), it should geometrically enhance construction of regular hydrogen-bond networks (such as that in hexagonal or cubic ice I) which utilize local tetrahedral symmetry to span space periodically. This angle distortion is small, but one recognizes that many chemical and physical processes in water hinge upon delicate interplay of competing effects. Under proper circumstances, then, small effects such as this one could produce large consequences.

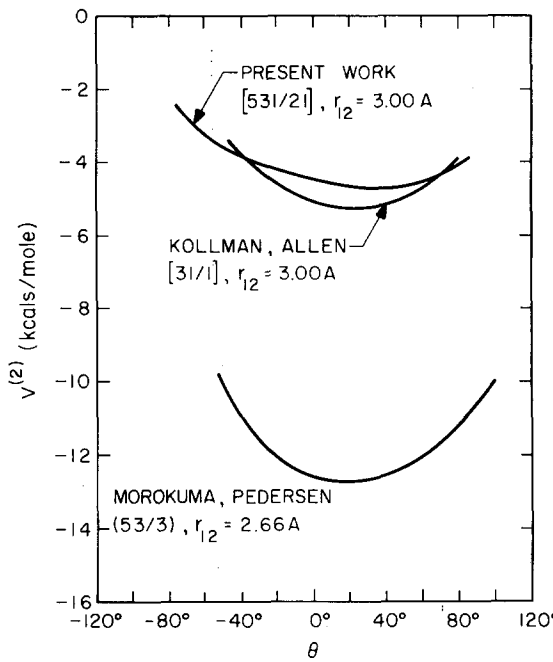

FIG. 3. Angular variation of $V^{(2)}$ for various basis sizes. The configurations are those illustrated in Fig. 1.

TABLE VII. Mullikan atomic populations and overlap values for water dimer.[a]

$R_{O_1O_2}=$	Atomic populations ∞	Atomic populations 3.00 Å	(3.00) − (∞)
Proton acceptor			−0.01136 (total)
O_1	8.64650	8.66862	0.02212
H_1	0.67675	0.66001	−0.01674
H_2	0.67675	0.66001	−0.01674
Proton donor			0.01135 (total)
O_2	8.64650	8.68426	0.03776
H_3	0.67675	0.64071	−0.03604
H_4	0.67675	0.68638	0.00963
	Overlaps		
$O_1\cdots H_3$	0.00000	0.01118	0.01118
H_3–O_2	0.67771	0.69724	0.01953
$O_1\cdots O_2$	0.00000	−0.01428	−0.01428
O_2–H_4	0.67771	0.68543	0.00772
O_1–H_1	0.67771	0.68079	0.00308

[a] Symmetric configuration of Fig. 1 with $\theta=40°$.

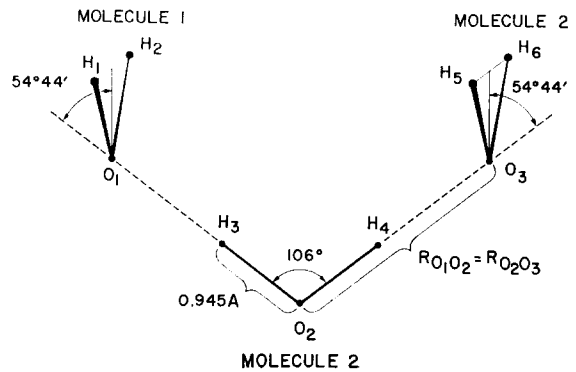

FIG. 4. Double donor trimer.

The oxygen d orbitals and hydrogen p orbitals that have been included in our basis seem to play an important role in determining the shape of angle-variation curves of the type shown in Fig. 2. Curve A from that figure is repeated in Fig. 3, along with equivalent angle-variation curves from Refs. 1 and 2. These latter computations did not include such polarization functions, and their results are much more nearly parabolic. The more extensive present basis produces a substantial, nearly linear, region roughly between $\pm 40°$. Curve B in Fig. 2 likewise shows a very flat portion in the same θ range, which we strongly suspect would not obtain with the smaller basis calculations.

It has been argued[23,24] that the dipole moment of the water molecule in ice should be 40% to 100% larger than its value for an isolated molecule. The mechanisms that produce this enhancement presumably operate as well in liquid water, though possibly with diminished effectiveness. Complete quantitative analysis of this phenomenon is beyond the scope of the present paper, even within the Hartree–Fock approximation. Still, the computed dimer structure reveals the beginning of this enhancement. In the minimum energy configuration of Fig. 1 for which $\theta=40°$ and $R_{O_1O_2}=3.00$ Å, the resultant dipole moment exceeds the vector sum of the component monomer moments in magnitude by 11%. Similar observations have been reported by Kollman and Allen[2] and by Diercksen.[13]

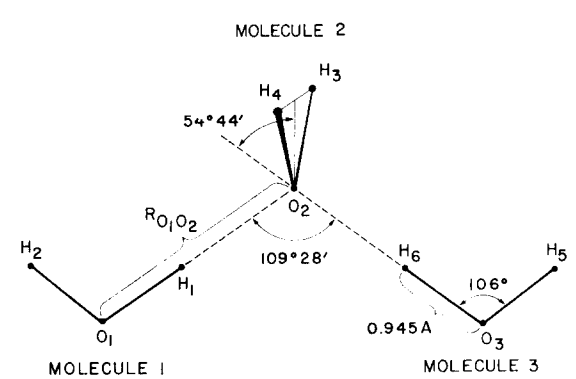

FIG. 5. Double acceptor trimer.

Mulliken atomic populations and overlap values[15] reflect charge redistribution in the dimer which underlies the dipole enhancement. Table VII displays these quantities in the same $\theta=40°$, $R_{O_1O_2}=3.00$ Å minimum energy configuration of Fig. 1. The entries in this table not only demonstrate charge transfer from the proton acceptor molecule to the proton donor, but show that the hydrogen bond has some covalent character.

Del Bene and Pople[19] infer from their calculations that the minimum-energy configuration for a dimer actually involves a slight hydrogen-bond nonlinearity. In terms of Fig. 1, they predict that molecule 2 should be rotated counterclockwise about O_2 by about 0.5°. This effect would seem to make sense in terms of repulsions acting between partially shielded protons. We have searched for this effect at the $\theta=40°$, $R_{O_1O_2}=3.00$ Å energy minimum for our own more extensive basis by interpolating between $\pm 5°$ rotation calculations (plus the undistorted case); no such nonlinearity was obtained however.

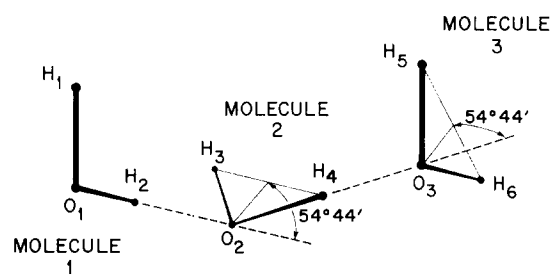

FIG. 6. Sequential trimer.

IV. TRIMER CALCULATIONS

In each of the ice polymorphs[17] and the clathrate hydrates,[18] water molecules invariably engage in four simultaneous hydrogen bonds. Two neighbors of a given molecule donate single protons to it, while its own protons are donated to two other near neighbors. At least in their ideal defect-free forms, therefore, these crystals all involve precisely two hydrogen bonds per water molecule.

Three distinct classes of hydrogen-bond triplets (trimers) occur in these crystals, that correspond to the distinct ways of selecting a molecule and two near neighbors. First, we have a "double acceptor" case, in which the central molecule and its two proton donor neighbors are chosen. Inversely, the central molecule plus the two neighbors to which it donates protons constitute a "double donor" trimer. Finally, the central molecule plus one of each neighbor type form a "sequential" trimer: one neighbor gives its proton to the central molecule, which in turn gives a proton to the second near neighbor. One can expect the three-body potential $V^{(3)}$ to behave rather differently for each of these three classes of trimers.

TABLE VIII. Trimer interaction energies and nonadditivities.[a]

	R_{OO} (Å)	θ (deg)	$E(1,2,3)$ $-3E(1)$	$V^{(2)}(1,2)$	$V^{(2)}(2,3)$	$V^{(2)}(1,3)$	$V^{(3)}(1,2,3)$
Sequential	2.76	−54.7	−6.766	−2.398	−2.398	−0.609	−1.363
	3.00	−54.7	−8.293	−3.433	−3.433	−0.433	−0.994
	3.15	−54.7	−7.949	−3.364	−3.364	−0.359	−0.863
	3.00	+54.7(1,2) −54.7(2,3)	−9.806	−3.433	−4.639	−0.678	−1.056
Double donor	2.76	−54.7	−2.973	−2.398	−2.398	0.947	0.874
	3.00	−54.7	−5.948	−3.433	−3.433	0.735	0.184
	3.15	−54.7	−6.141	−3.364	−3.364	0.627	−0.048
Double acceptor	2.76	−54.7	−3.140	−2.398	−2.398	1.310	0.346
	2.90	−54.7	−5.294	−3.241	−3.241	1.080	0.109
	3.00	−54.7	−5.965	−3.433	−3.433	0.950	−0.048
	3.15	−54.7	−6.120	−3.364	−3.364	0.791	−0.184
	3.39	−54.7	−5.456	−2.872	−2.872	0.607	−0.319
Asymmetric double acceptor	3.00	−54.7(1,2) −25 (2,3)	−5.489	−3.433	−4.092	1.967	0.069
	3.00	−54.7(1,2) −70 (2,3)	−5.484	−3.433	−2.756	0.761	−0.056

[a] All energies are in kilocalories per mole.

The occurrence frequencies of the three trimer classes are invariant for all ices and clathrates. Of the six trimers per molecule in these crystals there is one each of the "double donor" and "double acceptor" varieties. The remaining four are all "sequential."

Although the regular ice lattice undergoes a severe disruption through the melting transition, available evidence indicates that substantial hydrogen bonding remains in the liquid. Some bonds are broken upon melting, and those which remain are surely subject to varying degrees of strain. Still, substantial short-range order must persist in the liquid which is closely related to that of the solid. One can therefore safely assume that the above three classes of trimers occur often in the liquid with about the same 1:1:4 relative frequency for double donor, double acceptor, and sequential trimers that obtains in the solid.

Our trimer calculations have examined each of these three classes, though not so extensively as one might have wished. Figures 4, 5, and 6 show, respectively, the specific double donor, double acceptor, and sequential trimers utilized. The constituent molecules were always undistorted from the geometry predicted for the monomer with this basis set.

Table VIII contains the total trimer interaction energies, the constituent pair potentials, and the resulting nonadditivities. These trimers all involve two linear H bonds with equal lengths. The bulk of the results refers to simultaneous H-bond length changes along the ideal tetrahedral directions specified in Figs. 4–6; however, the last two entries in Table VIII entail an asymmetric variation in direction of H-bond approach (still linear) at constant bond length.

For the sake of clarity, the set of results for $V^{(3)}$ is depicted graphically in Fig. 7, for all cases in which the H-bond angles θ are uniformly $-54.7°$. The important feature illustrated by the curves is the variability of $V^{(3)}$ among the trimer classes. At least for the special configurations shown, the double donor and double acceptor trimers are somewhat energetically destabilized around the ice distance (2.76 Å), while the more numerous sequential trimers are strongly stabilized. Furthermore, the weighted sum of slopes at 2.76 Å is positive, which indicates a net compressive effect on an extended H-bond network.

Although the specific trimers for which curves in Fig. 7 are relevant occur in both hexagonal and cubic ice modifications, other trimers occur as well. These others may be obtained by rotation of molecules about the linear H bonds. Before attempting to draw quantitative conclusions about the effect of $V^{(3)}$ on the binding in these ices, it is obvious that these remaining trimers should be investigated. Practical considerations have not allowed us to exhaust the possibilities, but Table VIII includes one very suggestive entry, the last one under "Sequential." This configuration at 3.00 Å was obtained from its predecessor at the same distance by a 180° rotation of the end donor about its H bond.

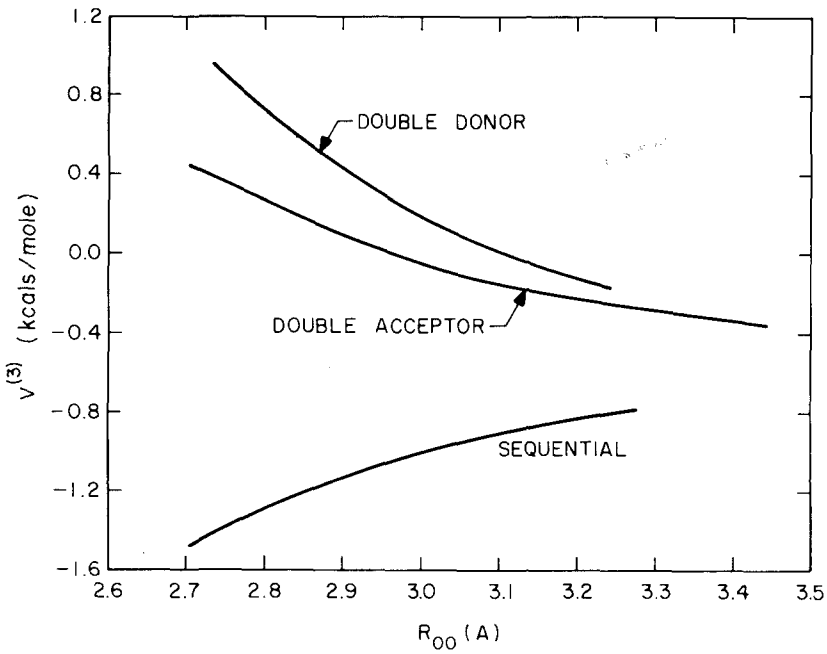

FIG. 7. Distance variation of trimer nonadditivity $V^{(3)}$. For each of the three classes shown, the component H-bonded dimers have $\theta = -54.7°$, exactly as shown in Figs. 4–6.

The final trimer so obtained is an expanded version of one that fits into hexagonal ice. But although the total trimer interaction energy changes substantially due to this rotation (−0.573 kcal/mole of trimers), $V^{(3)}$ changes very little (−0.062 kcal/mole of trimers). We interpret this to mean that $V^{(3)}$ is generally insensitive to bond rotations.

If this presumption of bond-rotation insensitivity is valid, we may use the results in Fig 7 to assess numerically the role of $V^{(3)}$ in the binding energy of ice. The result is[25]

$$4(-1.363)+1(0.874)+1(0.346)=-4.232 \text{ kcal/mole}$$

for the trimer contribution to the binding energy. A similar estimate for the rate of change of trimer nonadditivity with lattice constant R_{OO} gives

$$4(1.96)+1(-3.72)+1(-1.76)=2.36 \text{ kcal/mole}\cdot\text{Å},$$

a considerable compressive effect. Although it is possible that the aggregate influence of $V^{(4)}$, $V^{(5)}$,$\cdots$, could counterbalance this influence somewhat, we believe that this compression plays an important role in all ices and clathrate-type hydrates.

Mutatis mutandis, the same enhanced binding energy and compressive effects of trimer nonadditivity should apply in liquid water around room temperature and pressure. One can reasonably expect that in the configurationally disordered liquid H bonds frequently deviate from linearity and tetrahedral directions of donor approach. It is important to know if nonaddivity effects enhance these distortions in the liquid, or resist them.

An asymmetric angular distortion is reported in Table VIII for the double acceptor trimer. The component H bonds remain linear with length 3.00 Å, but the angle θ for pair (2, 3) is varied. So far as that variation is concerned, the pair (2, 3) undergoes precisely the same geometric change that is involved for $V^{(2)}$ in Fig. 2, curve A.

Figure 8 shows $V^{(2)}(2,3)$ along with the sum $V^{(2)}(2,3)+V^{(3)}(1,2,3)$. The latter combination reflects the indirect influence of the already formed H bond between (1, 2) along the tetrahedral direction. The resulting minimum in this composite angle curve is further evidence that formation of one tetrahedral bond increases sp^3 hybridization in the acceptor molecule. Though the minimum occurs around −20°, rather than the ideal tetrahedral angle −54.7°, the increased directionality is clear. If our hypothesis of $V^{(3)}$ transferability is correct, then the angular variation of $V^{(2)}(2,3)+V^{(3)}(1,2,3)$ for the double acceptor in which (2, 3) had the type of configuration represented in Fig. 2, curve B, would be closer to tetrahedral directionality. Thus it appears that $V^{(3)}$ tends to reinforce local tetrahedral coordination in condensed aqueous phases.

V. DISCUSSION

(1) It is appealing to suppose[23] that interaction nonadditivity might be explained merely on the basis of classical electrostatics. After all, electrostatic polarization energies in an assembly of polarizable point particles have nonadditive components. The simplest model that might reasonably be applied would treat each water molecule as a polarizable point bearing a permanent dipole moment. The obvious position for this "point" is the electrical center of the molecule, i.e., the position at which the axial quadrupole moment

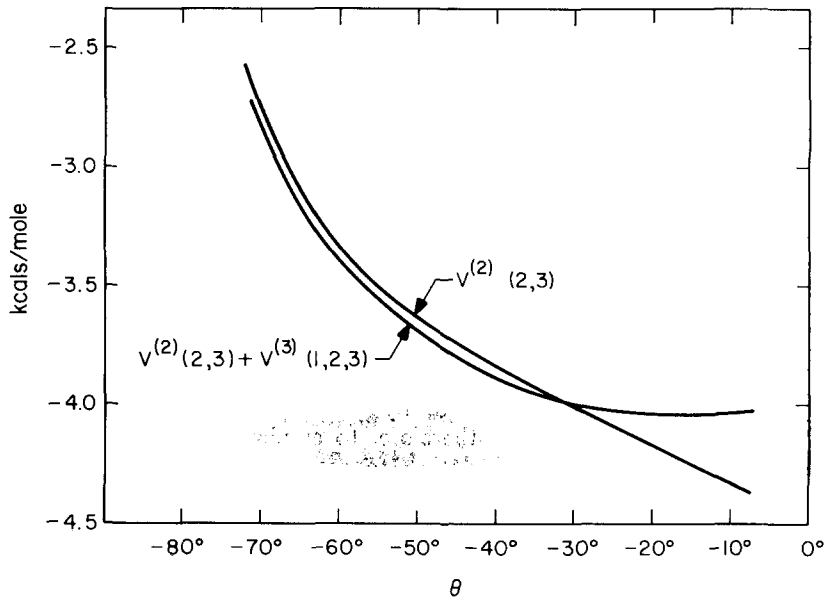

FIG. 8. $V^{(2)}(2, 3)$ and $V^{(2)}(2, 3)+V^{(3)}(1, 2, 3)$ for asymmetric angle variation in the double acceptor trimer ($R_{OO}=3.00$ Å).

vanishes. For our [531 | 21] wavefunction, this point lies 0.049 Å ahead of the oxygen nucleus, along the ∢HOH bisector. If this electrostatic basis for $V^{(3)}$, $V^{(4)},\cdots$, were valid, the nonadditivities for the double donor shown in Fig. 4 and the double acceptor trimer in Fig. 5 would be essentially the same. However we have seen in Fig 7 that the quantum mechanically computed $V^{(3)}$ values for these trimers differ by more than a factor of 2 at the ice lattice distance. One is forced to conclude that electrostatic models are inappropriate under condensed-phase density conditions.

(2) The effective pair interaction $v(i,j)$ is defined by minimizing the square error in the difference ($\beta=1/k_BT$),

$$\exp[-\tfrac{1}{2}\beta V_N(1\cdots N)]-\exp[-\tfrac{1}{2}\beta\sum_{i<j=1}^{N}v(i,j)] \quad (5.1)$$

between Boltzmann factors for the actual N-molecule potential V_N and the pairwise v-sum effective potential, over the entire accessible configuration space.[10] To the extent that $V^{(3)}$ contributions to the actual potential dominate all nonadditivity effects, we can tentatively conclude what the nature of the difference between $V^{(2)}$ and v should be. Since trimer effects add extra binding energy, the absolute minimum of v should lie at lower energy than the absolute $V^{(2)}$ minimum. Furthermore the v minimum should occur at a shorter R_{OO} distance than for $V^{(2)}$ due to the net trimer compression effect. Also v should exhibit more pronounced directionality for H-bond formation near the ideal tetrahedral directions due to enhanced hybridization in condensed phases. Finally, at the second-neighbor distance ($R_{OO}\cong 4.7$ Å), $v-V^{(2)}$ should be positive when the two molecules are oriented so both may donate or both receive protons from a third molecule but $v-V^{(2)}$ should be negative when they are so oriented that the third molecule may donate to one and accept from the other.

(3) The strongly negative values obtained for sequential trimer $V^{(3)}$'s (and the consequent over-all increase in binding energy) confirm Frank's concept of cooperativity in H-bond formation.[6,7] Potential nonadditivity therefore acts to keep ice solid above the melting point for "hypothetical ice" in which only the $V^{(2)}$'s were operative. But the fact that $V^{(3)}$ contributions boost the melting temperature of real ice does not at the same time imply that after melting, large icelike clusters should remain in the liquid. The existence of such clusters or "icebergs" is ruled out by the short-range nature of the experimental radial distribution function,[21] and by the fact that liquid water may be easily supercooled.

(4) The correlation energy error incurred by accurate Hartree–Fock calculations on water is unquestionably large. However, this error is primarily intramolecular, and should therefore be confined to $E^{(1)}$ largely.[26] Correlation effects in $V^{(2)}$ would reflect the dispersion attraction due to intermolecular correlated multipole fluctuations. This would be roughly equal to the neon dispersion attraction (Ne is isoelectronic with water), times the square of the water-to-neon polarizability ratio. We therefore estimate an additional binding energy, at 2.76-Å distance between the oxygens, of 0.9 kcal/mole. This extra binding should furthermore be quite undirectional, and thus should not affect the predicted linearity of the H bond. An analogous measure for the influence of electron correlation on $V^{(3)}$ is provided by the Axilrod–Teller three-body interaction.[27] Although the magnitude of this interaction is difficult to estimate for water, its angular variation is known, and is once again far less sensitive to rotations than the Hartree–Fock three-molecule energy itself. Furthermore, this Axilrod–Teller function will be negative and essentially constant (at fixed R_{OO} distances) for all three classes of H-bond trimers. Evidently the

class distinctions are properly established in the Hartree–Fock approximation, and are little affected by correlation.

(5) Several aspects of the water interaction problem deserve future study. It is desirable, for example, to carry out one or two tetramer calculations (with ice-lattice structure, most profitably) to establish if $V^{(4)}$ tends to be small. If this is so, then Eq. (1.1) is an especially apt way of representing the aggregate interaction for many-molecule assemblies. Del Bene and Pople[5,19] suggest that the most stable configuration for three water molecules involves a cyclic structure with three severely bent H bonds. Such triangular groupings are never observed in the ices or hydrate crystals, however. It would be useful, therefore, to employ a large-basis Hartree–Fock calculation to see if their trimer is spuriously stabilized by the orbital overlap effect mentioned in Sec. III. If it is not, the nonoccurrence of the triangular grouping in solids must rest upon the over-all favorability of many-molecule networks which incorporate only larger H-bond polygons.

(6) The thermodynamic and structural differences between light and heavy water stem from the difference in degree of quantum mechanical zero-point vibrational motion of the respective molecules. These motions of course are primarily associated with the hydrogen nuclei, rather than the more massive oxygen nuclei. In order to provide a firm basis for a statistical-mechanical theory of isotope shifts in water, potential energy surfaces should ultimately be mapped for hydrogen nucleus motion both in the monomer, and in H-bonded dimers with a variety of conformations. The results should help explain, for example, why D_2O melts 3.81° higher than H_2O, whereas its density maximum occurs (at 1 atm) 7.2° higher.

(7) Finally, accurate Hartree–Fock calculations would be invaluable for aqueous solution theory by providing potential energy curves between a water molecule and various solutes. It should be possible to establish characteristic behaviors for chemically distinct groupings (such as methyl groups, alcohol hydroxyls, amine groups, carbonyls, carbon double bonds, etc.) near a water molecule. One ultimately would be able to explain the hydration of complicated biopolymers, and thus contribute to deeper understanding of the physical chemistry of terrestrial life.

* The portion of this work carried out at N. Y. U. was partly supported by National Science Foundation grant GP-10331.

† To whom reprint requests should be directed.

[1] K. Morokuma and L. Pederson, J. Chem. Phys. **48,** 3275 (1968).
[2] P. A. Kollman and L. C. Allen, J. Chem. Phys. **51,** 3286 (1969).
[3] K. Morokuma and J. R. Winick, J. Chem. Phys. **52,** 1301 (1970).
[4] Some early results obtained in this project were reported in D. Hankins, J. W. Moskowitz, and F. H. Stillinger, Chem. Phys. Letters **4,** 527 (1970).
[5] J. Del Bene and J. A. Pople, Chem. Phys. Letters **4,** 426 (1969).
[6] H. S. Frank and W. Y. Wen, Discussions Faraday Soc. **24,** 133 (1957).
[7] H. S. Frank, Proc. Roy. Soc. (London) **A247,** 481 (1958).
[8] W. W. Wood, J. Chem. Phys. **48,** 415 (1968).
[9] B. J. Alder and T. E. Wainwright, J. Chem. Phys. **33,** 1439 (1960).
[10] F. H. Stillinger, J. Phys. Chem. **74,** 3677 (1970).
[11] D. Neumann and J. W. Moskowitz, J. Chem. Phys. **49,** 2056 (1968).
[12] C. C. J. Roothaan, Rev. Mod. Phys. **23,** 69 (1951).
[13] G. H. F. Diercksen, Chem. Phys. Letters **4,** 373 (1969).
[14] S. P. Liebmann (unpublished).
[15] R. S. Mulliken, J. Chem. Phys. **23,** 1833 (1955).
[16] That this feature should obtain has been stressed in R. F. W. Bader, J. Am. Chem. Soc. **86,** 5070 (1964).
[17] D. Eisenberg and W. Kauzmann, *The Structure and Properties of Water* (Oxford U. P., New York, 1969), Chap. 3.
[18] G. A. Jeffrey and R. K. McMullan, Progr. Inorg. Chem. **8,** 43 (1967).
[19] J. Del Bene and J. A. Pople, J. Chem. Phys. **52,** 4858 (1970).
[20] G. C. Pimentel and A. L. McClellan, *The Hydrogen Bond* (W. H. Freeman, San Francisco, 1960).
[21] A. H. Narten and H. A. Levy, Science **165,** 447 (1969).
[22] C. A. Coulson, *Valence* (Oxford U. P., New York, 1961), Chap. VIII.
[23] C. A. Coulson and D. Eisenberg, Proc. Roy. Soc. (London) **A291,** 445 (1966).
[24] L. Onsager and M. Dupuis, in *Electrolytes,* edited by B. Pesce (Pergamon, New York, 1962), p. 27.
[25] We assume that the effect is confined primarily to nearest-neighbor trimers in the crystal.
[26] L. C. Snyder (unpublished) estimates the $E^{(1)}$ correlation error to be 231±6 kcal/mole for water.
[27] B. M. Axilrod and E. Teller, J. Chem. Phys. **11,** 299 (1943).